Microbiome

RESEARCH

Open Access

Host-specific effects of *Eubacterium* species on Rg3-mediated modulation of osteosarcopenia in a genetically diverse mouse population

Soyeon Hong[1†], Bao Ngoc Nguyen[2,3†], Huitae Min[3], Hye-Young Youn[3], Sowoon Choi[3], Emmanuel Hitayezu[4], Kwang-Hyun Cha[4,5,6], Young Tae Park[3,5], Choong-Gu Lee[4,5,6], GyHye Yoo[1,5*] and Myungsuk Kim[3,5,6*]

Abstract

Background Osteosarcopenia, characterized by the simultaneous loss of bone and muscle mass, is a serious health problem in the aging population. This study investigated the interplay between host genetics, gut microbiota, and musculoskeletal health in a mouse model of osteosarcopenia, exploring the therapeutic potential of gut microbiota modulation.

Methods We examined the effects of Rg3, a phytochemical, on osteosarcopenia and its interactions with host genetics and gut microbiota in six founder strains of the Collaborative Cross (CC) population. Subsequently, we evaluated the therapeutic potential of Eubacterium nodatum (EN) and Eubacterium ventriosum (EV), two gut microbes identified as significant correlates of Rg3-mediated osteosarcopenia improvement, in selected C57BL/6 J (B6) and 129S1/SvImJ (129S1) mouse strains.

Results Rg3 treatment altered gut microbiota composition aligned with osteosarcopenia phenotypes, which response varied depending on host genetics. This finding enabled the identification of two microbes in the *Eubacterium* genus, potential mediator of Rg3 effect on osteosarcopenia. Oral administration of EN and EV differentially impacted bone density, muscle mass, exercise performance, and related gene expression in a mouse strain-specific manner. In 129S1 mice, EN and EV significantly improved these parameters, effectively reversing osteosarcopenic phenotypes. Mechanistic investigations revealed that these effects were mediated through the modulation of osteoblast differentiation and protein degradation pathways. In contrast, EN and EV did not significantly improve osteosarcopenic phenotypes in B6 mice, although they did modulate mitochondrial biogenesis and microbial diversity.

Conclusions Our findings underscore the complex interplay between host genetics and the gut microbiota in osteosarcopenia and emphasize the need for personalized treatment strategies. EN and EV exhibit strain-specific therapeutic effects, suggesting that tailoring microbial interventions to individual genetic backgrounds may be crucial for optimizing treatment outcomes.

†Soyeon Hong and Bao Ngoc Nguyen contributed equally to this work.

*Correspondence:
GyHye Yoo
loshell@kist.re.kr
Myungsuk Kim
g-sstainer@kist.re.kr
Full list of author information is available at the end of the article

Graphical Abstract

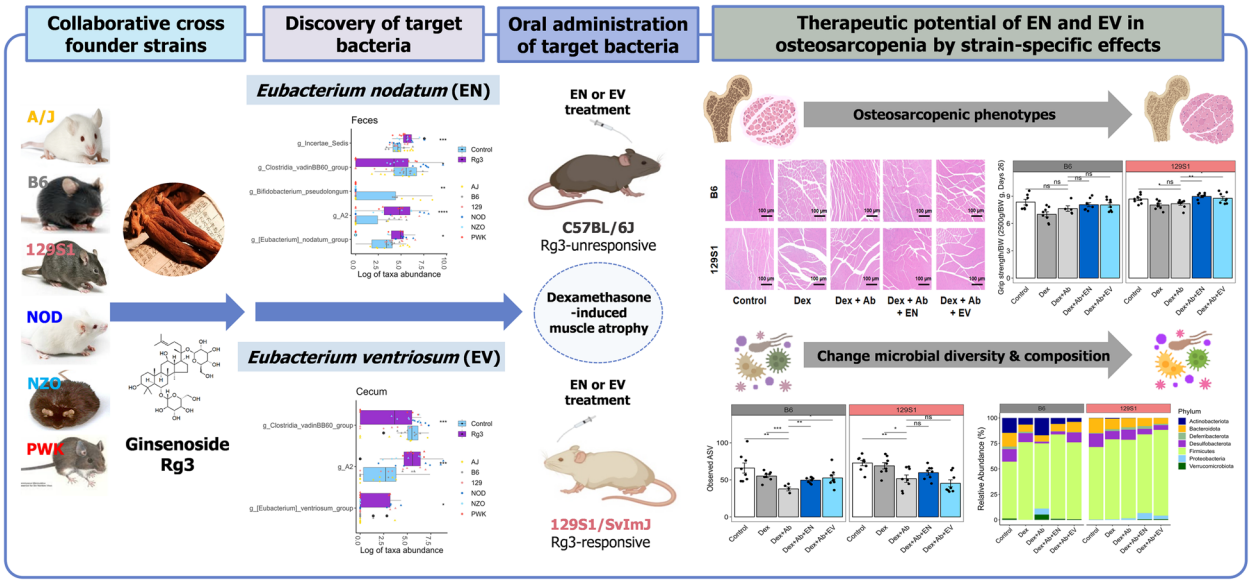

Background

Osteosarcopenia, characterized by a concurrent decline in muscle and bone mass with age, has emerged as a significant and escalating global public health concern. With rising life expectancy, the projected prevalence of osteosarcopenia is anticipated to increase dramatically, imposing a substantial burden on healthcare systems due to the elevated risk of falls, fractures, and limitations in functional mobility of patients [1]. However, there are currently no treatment options for osteosarcopenia approved by the Food and Drug Administration, highlighting the critical need to develop novel therapeutic strategies [2].

The etiology of osteosarcopenia likely involves a complex interplay between genetic and environmental factors. Genetic predisposition plays a significant role in osteosarcopenia, with specific gene variants conferring increased susceptibility to the syndrome [3, 4]. Methyltransferase like 21C, myocyte enhancer factor-2, and sterol regulatory element-binding transcription factor 1 have been well studied as candidate genes that are highly correlated with osteosarcopenia incidence [5–7]. Concurrently, environmental factors such as dietary patterns and gut microbiome composition also contribute to the disease process [8, 9]. Recent studies have highlighted a strong correlation between the gut microbiome and skeletal health [10–12], demonstrating that specific gut microbes or fecal microbiota transplantationcan influence both muscle [13, 14] function and bone integrity [14, 15, 16]. The environmental factors with the highest correlation with the disease were low potassium levels, alcohol consumption, low serum vitamin D levels, and immune factors [3]. However, dissecting the independent and interactive effects of these factors remains challenging.

Pharmacogenomics, a field dedicated to understanding how individual genetic variations influence drug responses, holds immense promise for the development of personalized treatment strategies for osteosarcopenia [17]. Traditional inbred mouse strains offer limited genetic variability, which hinders the generalizability of research findings in a broader human population [18]. To overcome this limitation, researchers are increasingly using genetically diverse mouse models, such as Collaborative Cross (CC) and Diversity Outbred populations. These genetically diverse mouse populations mirror the rich genetic heterogeneity found in humans, enabling a more comprehensive investigation of the complex interplay between genes and their environment [19, 20]. These models have proven valuable in studying the influence of genetic background on the response to various medications, including phytochemicals, in diseases such as obesity and diabetes [21–24]. Our previous research has elucidated the strain-dependent efficacy of Rg3 in osteosarcopenia models, highlighting the influence of host genetics on its therapeutic response [25]. Additionally, these models have been instrumental in identifying the influence of the genetic background on gut microbiota composition and homeostasis [26–28]. These findings highlight the importance of integrating

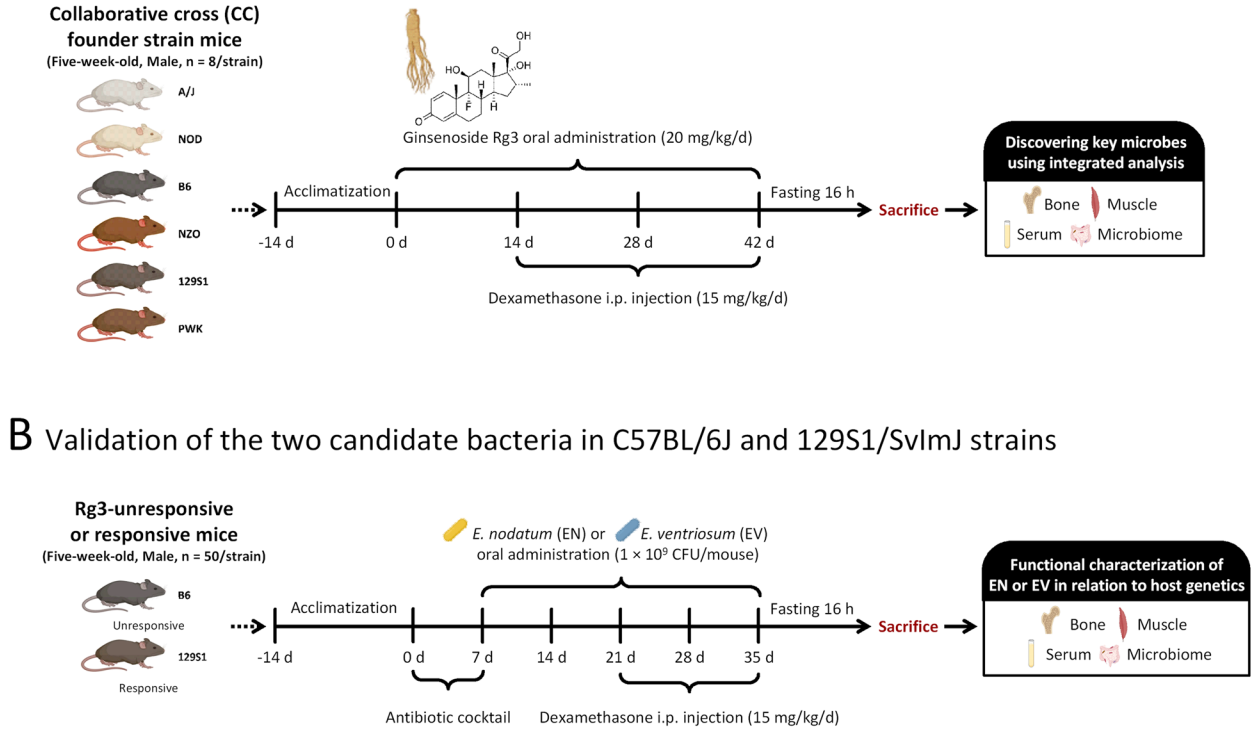

Fig. 1 Experimental design for two independent studies. **A** Experimental design for the collaborative founder strain study. **B** Experimental design for the validation study using C57BL/6 J and 129S1/SvImJ strains

pharmacogenomics with gut microbiome analyses in osteosarcopenia research. This combined approach holds promise for the development of personalized treatment strategies that consider both the genetic makeup and unique gut microbial composition of an individual.

Based on our previous research demonstrating the strain-dependent efficacy of Rg3, a phytochemical, in osteosarcopenia models [25], this study aimed to (1) investigate the mechanisms underlying the variable pharmacological effects of Rg3 across diverse genetic backgrounds, and (2) explore the therapeutic potential of gut microbiota modulation in osteosarcopenia. Leveraging the genetic diversity of CC founder strains, we examined the effects of Rg3, a well-characterized phytochemical with established pharmacological properties [29, 30], on osteosarcopenia and its interaction with host genetics, gut microbiota, and musculoskeletal health in six CC founder strains. This multifaceted approach led to the identification of *Eubacterium nodatum* (EN) and *Eubacterium ventriosum* (EV) as potential microbial targets. Subsequently, we evaluated the efficacy of EN and EV in reversing osteosarcopenia in selected mouse strains, aiming to elucidate the interplay between host genetics and gut microbiota in therapeutic responses.

Materials and methods

Bacterial media and cell culture conditions

Eubacterium nodatum (ATCC 33099; EN) and *Eubacterium ventriosum* (ATCC 27560; EV) were obtained from the American Type Culture Collection (ATCC, VA, USA) and cultivated in reinforced clostridial medium (RCM) under strict anaerobic conditions at 37 °C, per ATCC recommendations. After anaerobic cultivation, bacterial cultures were centrifuged, and the pellets were resuspended in sterile anaerobic phosphate-buffered saline for oral administration to mice.

Growth rate measurement

The growth rate of both bacteria was assessed in RCM under anaerobic conditions at 37 °C, both with and without Rg3 treatment. A 96-well plate reader (Multiskan SkyHigh; Thermo Fisher Scientific, MA, USA) was used for analysis. Each well was inoculated with a 1000-fold dilution of an overnight culture and subsequently treated with Rg3 in triplicate for each concentration. The cultures were incubated for 24 h with shaking at 200 rpm, and the optical density (OD) at 600 nm (OD600) was measured every 20 min. Exponential growth rates were calculated based on OD600 values between 0.02 and 0.1.

Animals: collaborative founder strains

The mouse experimental design is outlined in Fig. 1A. Five-week-old male mice ($n=8$/strain) from six strains, namely A/J, C57BL/6 J, 129S1/SvImJ, NOD/ShiLtJ, NZO/EiJ, and PWK/PhJ (referred to here as AJ, B6, 129S1, NOD, NZO, and PWK) were obtained from the Jackson Laboratory (Bar Harbor, ME, USA). Mice were housed under standard laboratory conditions with a 12-h light/dark cycle, controlled temperature, and humidity. They were allowed to acclimate to their new environment for 2 weeks before the start of the experiment. Following acclimatization, the mice from each strain were randomly assigned to either the control or Rg3 group ($n=4$/group). The control group received a vehicle control (0.5% CMC) orally, while the Rg3 group received Rg3 at a dose of 20 mg/kg/day via oral gavage for 6 weeks. After 2 weeks, all mice received intraperitoneal dexamethasone (DEX) injections (15 mg/kg/day) for 1 month to induce muscle atrophy and bone loss. Mice had ad libitum access to food and water throughout the study. After 6 weeks of Rg3 or vehicle administration and 16 h fasting, the mice were euthanized. Plasma, muscle (quadriceps, gastrocnemius, tibialis, and soleus), bone (femurs), spleen, cecum, and fecal samples were collected and stored at − 80 °C for further analysis. Muscle weight was measured using an analytical balance (Mettler Toledo, OH, USA), and the muscle-to-body weight ratio was calculated for atrophy assessment.

Animals: validation of the two candidate bacteria in C57BL/6 J and 129S1/SvImJ strains

The mouse experimental design is outlined in Fig. 1B. A total of 100 male mice, 50 of each strain (C57BL/6 J and 129S1/SvImJ), were obtained from the Jackson Laboratory at 5 weeks of age. All animal experimental protocols were approved by the International Animal Care and Use Committee of the Korea Institute of Science and Technology (KIST-2021–091002) and adhered to the established guidelines and regulations. The mice were housed under controlled conditions (25 °C, 45% humidity, 12-h light/dark cycle) and fed a standard AIN-76A diet with ad libitum access to water. Following acclimatization, the mice from each strain were randomly assigned to five groups ($n=10$/group): control, DEX, DEX + antibiotics, DEX + antibiotics + EN (DEX + EN), and DEX + antibiotics + EV (DEX + EV). Mice in the DEX + antibiotic groups received a 1-week broad-spectrum antibiotic cocktail [neomycin (1 g/L), ampicillin (1 g/L), vancomycin (0.5 g/L), metronidazole (0.5 g/L), imipenem (0.5 g/L), and ciprofloxacin (0.2 g/L)] in their drinking water before the administration of bacterial strains. EN and EV (1×10^9 CFU/mouse) were orally administered once daily for 4 weeks. All groups, except the control group, received intraperitoneal DEX injections for 2 weeks. Body weight was monitored every other day during DEX treatment. After 16 h of fasting, the quadriceps, gastrocnemius, soleus, and tibialis muscles were dissected, weighed (using an analytical balance with 0.01 mg sensitivity), and frozen in liquid nitrogen. The muscle-to-body weight ratio was used as the primary indicator of muscle atrophy.

Grip strength test and treadmill running exercise

The detailed mouse experimental design has been reported in our previous study [25]. Grip strength was measured using a Bioseb grip force meter (Pinellas Park, FL, USA), according to established protocols. Briefly, mice were placed on a grid and gently pulled by the tail in the opposite direction until their forelimbs were detached. The maximum force recorded during detachment was used as the grip strength score. Each mouse underwent three trials, with rest periods in between trials.

Endurance was assessed using a PanLab Touchscreen Treadmill (Harvard Apparatus, Holliston, MA, USA). Acclimatization involved a 15-min run at 10 m/min. The test started at 10 m/min and was gradually increased in increments of 1 m/min until exhaustion. A 20-V shock bar on the back of the treadmill deterred resting. The runtime and workload were recorded automatically. Exhaustion was defined as no movement for more than 10 s, and the total distance was calculated by multiplying the runtime and speed.

Histological analysis of skeletal muscle

Gastrocnemius muscles were immersed overnight in 4% formalin and subsequently embedded in paraffin. Tissue Sects. (5 μm) were stained with hematoxylin and eosin (H&E) using standard protocols. The muscle fiber cross-sectional area (CSA) was quantified using ImageJ software. For each muscle, five non-overlapping fields were randomly selected at 200 × magnification using a ZEISS microscope (Oberkochen, Germany). Within each field, the CSA of all muscle fibers was quantified using ImageJ software and expressed as a percentage of the mean of the control group.

ATP level measurement

ATP content in the tibialis muscle was assessed using a commercially available ATP content kit (DoGenBio, Seoul, Korea), following the manufacturer's protocol. The protein contents of the samples were normalized to account for potential variability. The absorbance was measured at 570 nm using a microplate reader.

Table 1 List of primers

Species	Target gene	Direction	Primer sequence (5′–3′)	Gene ID
Mouse	*Fbxo32*	Forward	AACCCTTGGGCTTTGGGTTT	NM_026346.3
		Reverse	GGACTTAAGCCCGTGCAGAT	
	Mstn	Forward	TGGCTCCTACTGGACCTCTC	NM_010834.3
		Reverse	AAGATGCAGCAGTCACTCCC	
	Trim63	Forward	GAGGGGCTACCTTCCTCTCA	NM_001039048.2
		Reverse	TTTACCCTCTGTGGTCACGC	
	Myog	Forward	AGCTATCCGGTTCCAAAGCC	NM_031189.2
		Reverse	GCACAGGAGACCTTGGTCAG	
	Myod	Forward	CATAGACTTGACAGGCCCCG	NM_010866.2
		Reverse	CGGGTCCAGGTCCTCAAAAA	
	Myf5	Forward	TCCAGGTATTCCCACCTGCT	NM_008656.5
		Reverse	TCAGCTTTGTGTGCTCCGAA	
	Myf6	Forward	ACAGATCGTCGGAAAGCAGC	NM_008657.3
		Reverse	CACTCCGCAGAATCTCCACC	
	Myog	Forward	AGCTATCCGGTTCCAAAGCC	NM_031189.2
		Reverse	GCACAGGAGACCTTGGTCAG	
	Myh2	Forward	AGCGAAGAGTAAGGCTGTCC	NM_001039545.2
		Reverse	AGGCGCATGACCAAAGGTT	
	Ppargc1a	Forward	GTTGCCTGCATGAGTGTGTG	NM_008904.3
		Reverse	CACATGTCCCAAGCCATCCA	
	Nrf1	Forward	CCCGTGTTCCTTTGTGGTGA	NM_001410231.1
		Reverse	ATTCCATGCTCTGCTGCTGG	
	Tomm20	Forward	TGTGCGGTGTGTTGTCTGTT	NM_024214.2
		Reverse	TAAGTGCCCAGAGCACAGGA	
	Tfam	Forward	GGGAATGTGGAGCGTGCTAA	NM_009360.4
		Reverse	TGCTGGAAGGTGGACAGTGAGG	
	Alpl	Forward	GATCATTCCCACGTTTTCAC	NM_001287172.2
		Reverse	TGCGGGCTTGTGGGACCTGC	
	Tnfrsf11b	Forward	CCGAGGACCACAATGAACA	NM_001411506.1
		Reverse	TCCTGGGTTGTCCATTCAA	

Muscle aconitase activity

Tibialis muscle samples were homogenized in cold radioimmunoprecipitation assay lysis buffer (500 µL/sample) using a homogenizer. Following homogenization, the samples were centrifuged at 13,000 rpm for 20 min. Aconitase activity in the supernatant was measured according to the manufacturer's protocol (Abcam, Cambridge, UK). Absorbance was measured at 575 nm for 30 min at 37 °C using a spectrophotometer.

Tibialis muscle and femur mRNA analysis

Total RNA was isolated from the tibialis muscle and left femurs using the Hybrid-R RNA purification kit (GeneAll Biotechnology, Seoul, Korea). cDNA synthesis was performed using the Reverse Transcription Premix (ELPIS-Biotech, Daejeon, Korea). qRT-PCR was performed on a LightCycler 480 Real-Time PCR System (Roche, Basel, Switzerland) using PowerUpTM SYBRTM Green Master Mix (Thermo Fisher Scientific) and gene-specific primers. Mouse β-actin was used as the endogenous control. Relative gene expression was calculated using the $2^{-\Delta\Delta Ct}$ method. The primer sequences are listed in Table 1.

Micro-computed tomography

Distal right femurs were collected and fixed in 4% paraformaldehyde (PFA). Each fixed distal femur was scanned using a SkyScan 1172 (Bruker Micro CT Corp., Kontich, Belgium). An image was acquired under 142 µA of source current and 70 kV of source voltage. The scanned bones were analyzed using Nrecon and CTAn integrated software (Bruker Micro CT Corp.) to estimate bone mineral density (BMD), bone surface area/bone volume (BS/BV), trabecular thickness (Tb.Th), trabecular spacing (Tb.Sp), trabecular plate number (Tb.N), bone surface area/total

volume (BS/TV), and bone volume/total volume (BV/TV).

Serum parameters of bone turnover

Blood samples were collected after an overnight fast. After centrifugation at 14,000 rpm for 30 min at 4 °C with the blood, 10 µL of serum was diluted 10 times and used. Serum osteocalcin (OCN) levels were measured using a Gla-type osteocalcin (Gla-OC) EIA Kit (TaKaRa Bio Inc., Japan). The absorbance was measured at 450 nm, and the analysis was performed as per the manufacturer's instructions.

16s rRNA gene sequencing of fecal and cecal samples

Following animal sacrifice, the feces and cecum were immediately frozen at − 80 °C until DNA extraction. Bead-beating homogenization was used to disrupt the samples, followed by DNA isolation using the QIAamp® Fast DNA Stool Mini Kit (Qiagen, Hilden, Germany). The V3-V4 region of the 16S rRNA gene was amplified via PCR using the universal primers 341F and barcoded 806R. Gel electrophoresis confirmed the PCR product amplicons, which were then purified using AMPure XT beads and quantified using Qubit dsDNA reagent. Sequencing was performed on an Illumina MiSeq platform using a paired-end 2 × 300 bp reagent kit. Raw data analysis was performed using the QIIME2-DADA2 pipeline to generate amplicon sequence variants (ASVs). Taxonomic classification (phylum to genus) was performed using the QIIME 2 software. Alpha (Shannon, Faith's PD, and observed ASVs) and beta (Unweighted Unifrac and Bray–Curtis) diversities were calculated using phyloseq and imported to R (v. 4.1.2) for analysis [30, 31]. Stacked bar plots depict taxon abundance at each classification level. ANCOM2.1 (significance threshold: ANCOM $W > 0.7$) was used for the differential abundance analysis of the genera.

Statistical analysis

R v4.1.2 (R Core Team) was used for all analyses. Differences between the control and Rg3 groups were evaluated using the Wilcoxon test. Efficacy data for EN and EV are presented as mean ± standard error of the mean (SEM). Group means were compared using one-way analysis of variance (ANOVA) followed by Tukey's post hoc test ($\alpha = 0.05$). For each strain, a two-way ANOVA ($\alpha = 0.05$) was used to assess the main effects (sample) and interactions (strain × sample) of muscle and bone health traits across all mice. This approach aimed to identify the influence of the genetic background on these traits. Spearman's rank correlation (*P*-values adjusted via Benjamini-Hochberg) was used to explore the relationships between microbial taxa abundance and other variables. Correlations were visualized using the "heatmap" package [32]. The differential abundance of genera was analyzed using ANCOM 2.1 [33] ($W > 0.7$ considered significant). Beta diversity was assessed using the nonparametric permutational multivariate ANOVA test (McArdle and Anderson, 2001) in the "vegan" package [34].

Results

Host genotype modulates Rg3-mediated shifts in gut microbial diversity and composition

Expanding on our previously reported strain-specific effects of Rg3 on musculoskeletal health in six DEX-treated CC founder strains [25], we investigated its influence on gut microbiome composition. Fecal and cecal samples were analyzed using 16S rRNA gene amplicon sequencing to elucidate the potential interactions between the host genotype and the effects of Rg3 on the gut microbiota. Consistent with prior observations using CC founder strains, 16S rRNA gene amplicon sequencing of fecal and cecal samples revealed significant host genotype effects on the gut microbiota composition at the phylum level (Fig. 2A, Table S1 and S2). Notably, minimal differences were observed between the sample sites (feces vs. cecum) for each strain. The NOD strain displayed a lower abundance of *Verrucomicrobiota*, including *Akkermansia muciniphila*, than did the other strains (Fig. 2A). Interestingly, the NZO strain, which is predisposed to polygenic obesity, exhibited a markedly elevated abundance of *Proteobacteria*, including *Escherichia-Shigella*, specifically in fecal samples (Fig. 2A, Table S1). This suggests potential compartment-specific effects on the microbiota. Conversely, the wild-derived PWK strain harbored the highest abundance of *Verrucomicrobiota* in both feces and cecum (Fig. 2A). Rg3 treatment further modulated gut microbiota composition in a genotype-dependent manner. In the NZO strain, Rg3 treatment significantly reduced the abundance of *Proteobacteria* (Fig. 2A). Conversely, Rg3 treatment increased the abundance of *Verrucomicrobiota* in PWK (Fig. 2A). These findings suggest complex interactions between host genotype, Rg3 treatment, and the resulting gut microbial profile.

Two-way ANOVA revealed significant effects of the strain and its interaction with the sample on alpha diversity indices (Shannon, Faith's PD, and observed ASVs) in both feces and cecum (Fig. 2B and S1B, Table S3 and S4). The NOD strain displayed the highest alpha diversity, whereas the PWK strain displayed the lowest alpha diversity (Fig. S2A and 2B). Rg3 treatment significantly

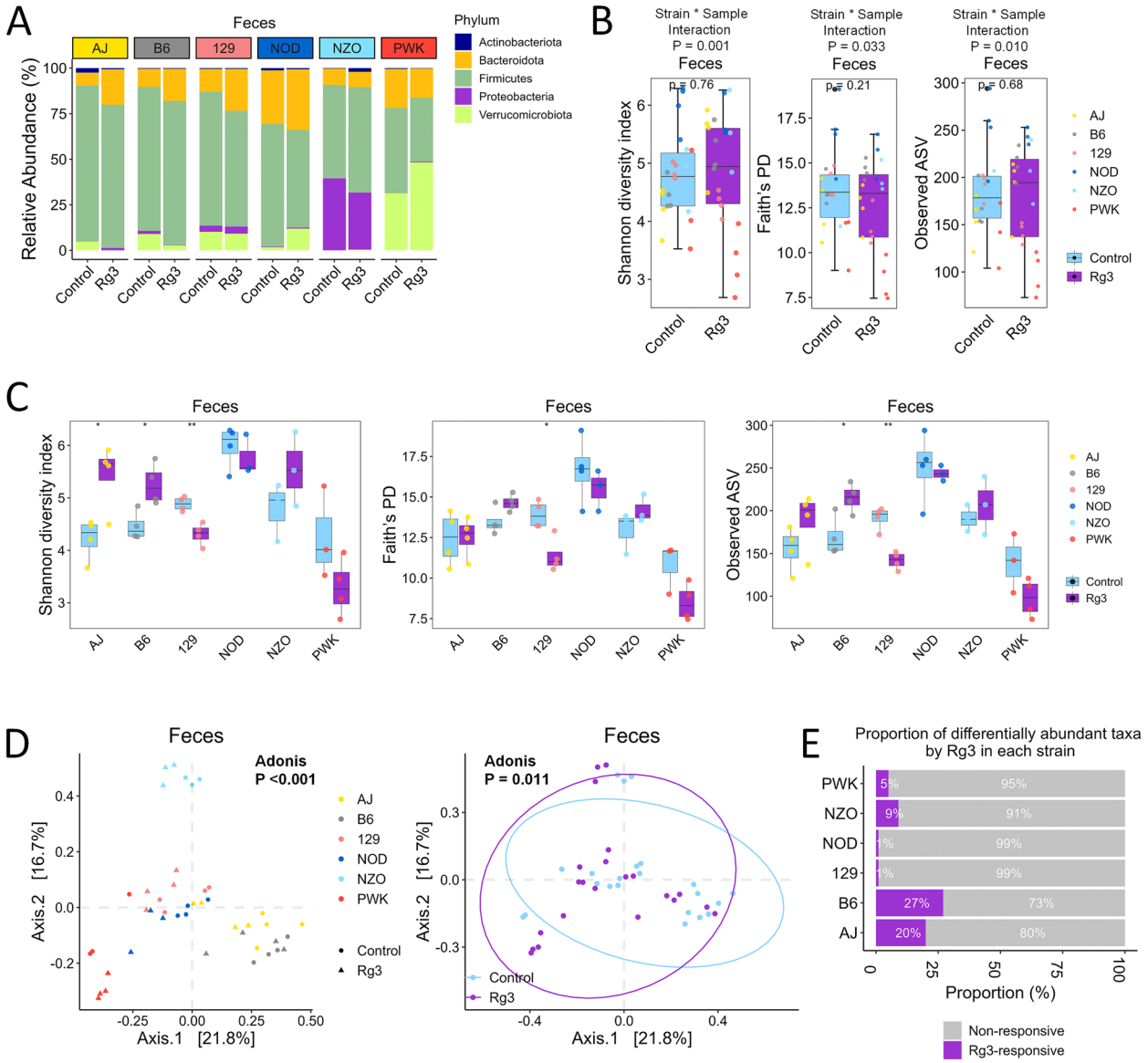

Fig. 2 Rg3 treatment alters fecal microbiota composition in six Collaborative Cross (CC) founder strains. **A** Relative abundance of gut microbiota at the phylum level following Rg3 treatment in the six CC founder strains. **B** Strain-by-treatment interaction boxplots for three alpha diversity metrics (Shannon diversity, Faith's PD, and observed ASV) following Rg3 treatment. **C** Comparison of alpha diversity metrics across the six founder strains with and without Rg3 treatment. Asterisks indicate statistically significant differences (*$p < 0.05$; **$p < 0.01$) as determined using Wilcoxon test. **D** Principal coordinate analysis (PCoA) plots depicting beta diversity of the gut microbiota in the six founder strains with and without Rg3 treatment. Symbols represent individual samples, and colors denote strain identity. **E** Proportion of differentially abundant taxa identified by Rg3 treatment within each strain. A/J (AJ); C57BL/6 J (B6); 129S1/SvImJ (129); NOD/ShiLtJ (NOD); NZO/HlLtJ (NZO); and PWK/PhJ (PWK)

reduced alpha diversity in the cecum but not in the feces, with strain-specific responses observed (Fig. 2B, C, S1B, and S1C). Beta diversity analysis confirmed significant differences in the microbial community composition across strains following Rg3 treatment (Table 2, Fig. 3D, S1D, S2C-F). Notably, the NZO and PWK strains displayed distinct profiles, and Rg3 treatment induced significant shifts in these profiles compared with those of the control group (Table 2, Fig. 2D, S1D). Additionally, the proportion of differentially abundant taxa following Rg3 treatment varied with the strain (Fig. 2E and S1E). Collectively, these results suggest that the host genotype significantly influences the effect of Rg3 treatment on gut microbiota diversity and bacterial abundance profiles.

Table 2 Multivariate homogeneity of groups dispersions (betadisper) and permutational multivariate analysis of variance (ADONIS) analysis of the microbial beta diversity between strains or treatment groups (control vs. Rg3) in six CC founder strains. $n = 44$ (22 mice for control and 22 mice for Rg3-treated mice). A/J (AJ); C57BL/6 J (B6); 129S1/SvImJ (129); NOD/ShiLtJ (NOD); NZO/HlLtJ (NZO); and PWK/PhJ (PWK)

Feces	β-dispersion		ADONIS		
	F	*P*	F. model	R^2	*P*
Strain effect					
Weighted UniFrac	1.715	0.158	11.546	0.603	**0.001**
Unweighted UniFrac	0.331	0.889	3.552	0.318	**0.001**
Bray–Curtis	1.366	0.263	8.834	0.538	**0.001**
Sample effect (Control vs Rg3)					
Weighted UniFrac	0.560	0.472	2.849	0.064	**0.029**
Unweighted UniFrac	7.999	**0.009**	1.899	0.043	**0.002**
Bray–Curtis	1.470	0.222	2.467	0.055	**0.011**
Cecum	**β-dispersion**		**ADONIS**		
	F	*P*	F. model	R^2	*P*
Strain effect					
Weighted UniFrac	0.985	0.434	10.389	0.578	**0.001**
Unweighted UniFrac	1.181	0.331	2.916	0.277	**0.001**
Bray–Curtis	1.524	0.223	9.080	0.544	**0.001**
Sample effect (Control vs Rg3)					
Weighted UniFrac	0.965	0.318	1.105	0.026	0.301
Unweighted UniFrac	0.346	0.559	1.780	0.041	**0.001**
Bray–Curtis	1.703	0.176	2.237	0.051	**0.021**

Gut microbiota diversity and Rg3-mediated genus-level changes correlate with muscle and bone phenotypes

Our previous study revealed that Rg3 exerted strain-dependent effects on muscle, bone, and immune functions [25]. In this study, we aimed to elucidate the potential contribution of gut microbiota to these Rg3-mediated phenotypes. Beta diversity analysis revealed that the fecal and cecal microbial community composition was significantly associated with muscle atrophy and bone loss-related phenotypes (Fig. 3A, B, and S3A). Notably, endurance capacity and bone mineral parameters showed the strongest correlations with alpha and beta diversity (Fig. S3B, S3C).

Next, we employed ANCOM to identify the differentially abundant bacterial genera in the feces and cecum following Rg3 treatment while controlling for strain effects. Rg3 treatment consistently decreased the abundance of *Clostridia vadin BB60* and increased that of *Lachnospiraceae bacterium A2* and *Eubacterium* in both compartments (Fig. 3C, D). Specific *Eubacterium* species, including EN and EV, exhibited significant changes in abundance across multiple strains after Rg3 treatment (Fig. 3E, F). For example, Rg3 administration increased EN in the feces of AJ and 129S1 strains, whereas it increased EV abundance in the cecum of 129S1, NOD, and PWK strains (Fig. 3F). These observations highlight the interplay between host genotype and Rg3 in shaping the abundance of specific bacterial genera.

Finally, we explored the correlation between Rg3-regulated genera and muscle atrophy/bone loss phenotypes. Among the identified genera (69 in feces and 54 in cecum), an abundance of *Akkermansia*, recognized for its muscle-protective properties [35], in both fecal and cecal samples, exhibited a positive correlation with

(See figure on next page.)

Fig. 3 Abundance of EN and EV and their association with osteosarcopenic phenotypes in CC founder strains. **A**, **B** Association between osteosarcopenic traits and variance in Bray–Curtis distance of fecal (**A**) and cecal (**B**) microbiota composition in six CC founder strains. Significant associations (*p*-values) are included in the bar graph. **C**, **D** Differentially abundant genera between control and Rg3 treatment for fecal (**C**) and cecal (**D**) microbiota in six CC founder strains. Colors represent the strain and sample information. Asterisks indicate statistically significant differences (*$p < 0.05$; **$p < 0.01$) determined using ANCOM2.1 and Wilcoxon test. **E**, **F** Effect of Rg3 on the relative abundance of EN and EV from all mice (**E**) and individual strains (**F**). **G**, **H** Spearman correlation plots between grip strength and bacterial abundance of (**G**) EN in the feces and (**H**) EV in the cecum by sample treatment. A/J (AJ); C57BL/6 J (B6); 129S1/SvImJ (129); NOD/ShiLtJ (NOD); NZO/HlLtJ (NZO); and PWK/PhJ (PWK)

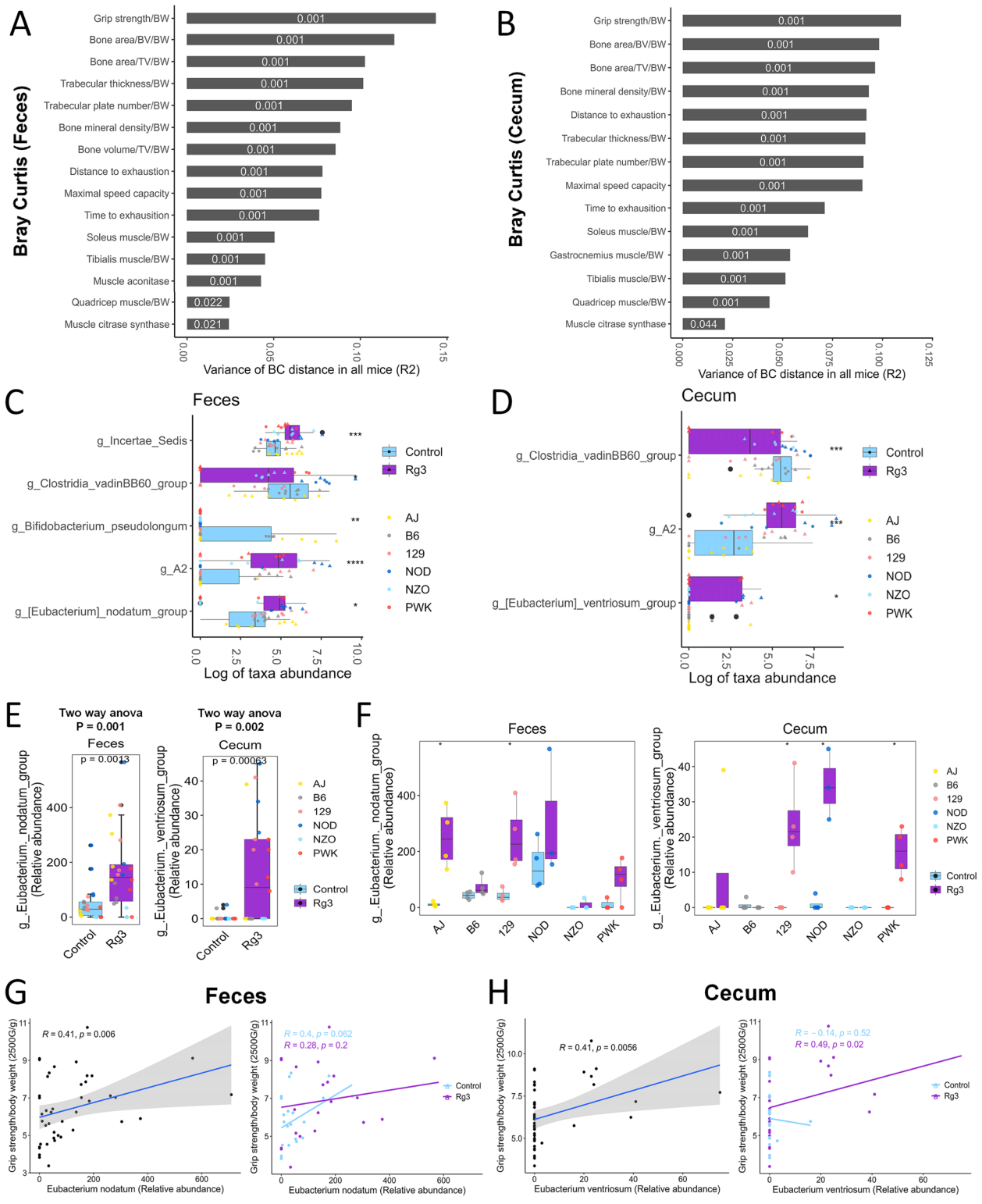

Fig. 3 (See legend on previous page.)

grip strength, irrespective of Rg3 treatment (Fig. S4A, S4C, S4D). Conversely, *Acetatifactor*, a genus known to produce potentially deleterious lithocholic acid [36], was negatively correlated with grip strength in both compartments (Fig. S4B, S4C, S4D). This association was more pronounced after Rg3 treatment. Interestingly, EN and EV, whose abundance increased after Rg3 treatment, were significantly correlated with grip strength in the feces and cecum, respectively. Notably, Rg3 treatment modulated the strength of these correlations (Fig. 3G, H).

Strain-dependent amelioration of muscle atrophy by EN and EV through inhibition of protein degradation pathways

Building on the identified association between EN/EV abundance and muscle atrophy phenotypes, we investigated the effects of EN and EV on muscle function and morphology in a DEX-induced muscle atrophy model using B6 and 129S1 mice. We aimed to elucidate whether the observed increase in EN/EV abundance after Rg3 treatment in 129S1 mice translated to enhanced muscle health compared with that in the reference B6 strain. In vitro analysis confirmed the ability of Rg3 to promote the growth of both EN and EV at concentrations up to 25 μM (Fig. S5). In vivo, a targeted antibiotic regimen was employed to identify relevant bacterial modulators within the gut microbiota. DEX treatment and antibiotic administration resulted in a significant body weight reduction in both mouse strains. Notably, administration of neither EN nor EV led to body weight recovery (Fig. S6A). Interestingly, compared with the antibiotic pretreatment group, EN and EV selectively enhanced average myofiber CSA in the gastrocnemius muscle (Fig. 4A, B), grip strength (Fig. 4C), muscle mass (Fig. 4D–F) of 129S1 mice compared with those in B6 mice. This effect was more pronounced with EN treatment. Two-way ANOVA revealed a significant interaction between strain and groups for grip strength and muscle mass (Fig. S6B–G), suggesting a potential genetic influence on the efficacy of these bacterial interventions in ameliorating muscle atrophy.

To explore the mechanisms underlying these strain-dependent phenotypic changes, we evaluated the expression of genes involved in protein degradation and myoblast differentiation. Similar to the observed muscle function and mass phenotypes, mRNA expression of the protein degradation markers *Fbxo32*, *Mstn*, and *Trim63* was decreased upon EN or EV treatment to a greater extent in the 129S1 strain than that in the B6 strain (Figs. 4G, H, S7A). Conversely, the expression of myogenic markers (*Myh2*, *Myod*, *Myog*, *Myf5*, and *Myf6*) generally increased following EN or EV treatment in the B6 strain (Fig. S7B–F). These findings suggest that EN and EV may exert their effects through distinct mechanisms in the two strains, with a greater emphasis on the inhibition of protein degradation pathways in the 129S1 strain and modulation of myogenic pathways in the B6 strain.

EN and EV promote bone health through modulation of osteoblast differentiation in a strain-dependent manner

Building on the observed strain-dependent effects of EN and EV on muscle health, we investigated their effects on bone health in B6 and 129S1 mouse models with DEX-induced osteoporosis. This experiment aimed to determine whether the potential benefits of EN or EV are modulated by the genetic background of the host. Similar to muscle atrophy-related phenotypes, DEX and antibiotic treatment resulted in significant bone loss in the 129S1 strain, as evidenced by the decreased BMD, BV, serum osteocalcin, Tb.Th, and Tb.N. (Fig. 5A–F). Notably, treatment with EN or EV mitigated these DEX-induced bone loss effects in the 129S1 strain (Fig. 5A–F). Analysis of the combined data from both strains indicated that both EN and EV significantly increased BMD, BA, Tb.N, and serum osteocalcin (Fig. S6H–N). However, a two-way ANOVA revealed a significant effect of strain on all bone loss-related phenotypes highlighting the potential for genetic modulation of these responses.

To gain further insights into the underlying mechanisms, we evaluated the expression of key osteoblast differentiation markers, namely *Alpl* (alkaline phosphatase) and *Tnfrsf11b* (osteoprotegerin). The expression patterns of these markers generally mirrored the observed bone phenotype data (Fig. 5G, H), further supporting the potential influence of EN and EV on osteoblast differentiation. However, the data also suggest a differential

(See figure on next page.)

Fig. 4 Effect of EN and EV on muscle atrophy markers in DEX-treated B6 and 129S1 mice. **A** Representative hematoxylin and eosin (H&E) staining of the gastrocnemius muscle and (**B**) quantification of the average muscle fiber cross-sectional area. **C** Grip strength normalized to body weight (**D**–**F**) and muscle weight relative to body weight for gastrocnemius (**D**), tibialis (**E**), and soleus (**F**) muscles. **G**, **H** Effect of EN and EV on mRNA expression of protein degradation markers (*Fbxo32* and *Trim63*) in DEX-treated B6 and 129S1 mice. Data are represented as mean ± SEM. Statistical significance was determined using one-way ANOVA followed by Tukey's post hoc test. *$p < 0.05$, **$p < 0.01$, ns (not significant). C57BL/6 J (B6); 129S1/SvImJ (129S1)

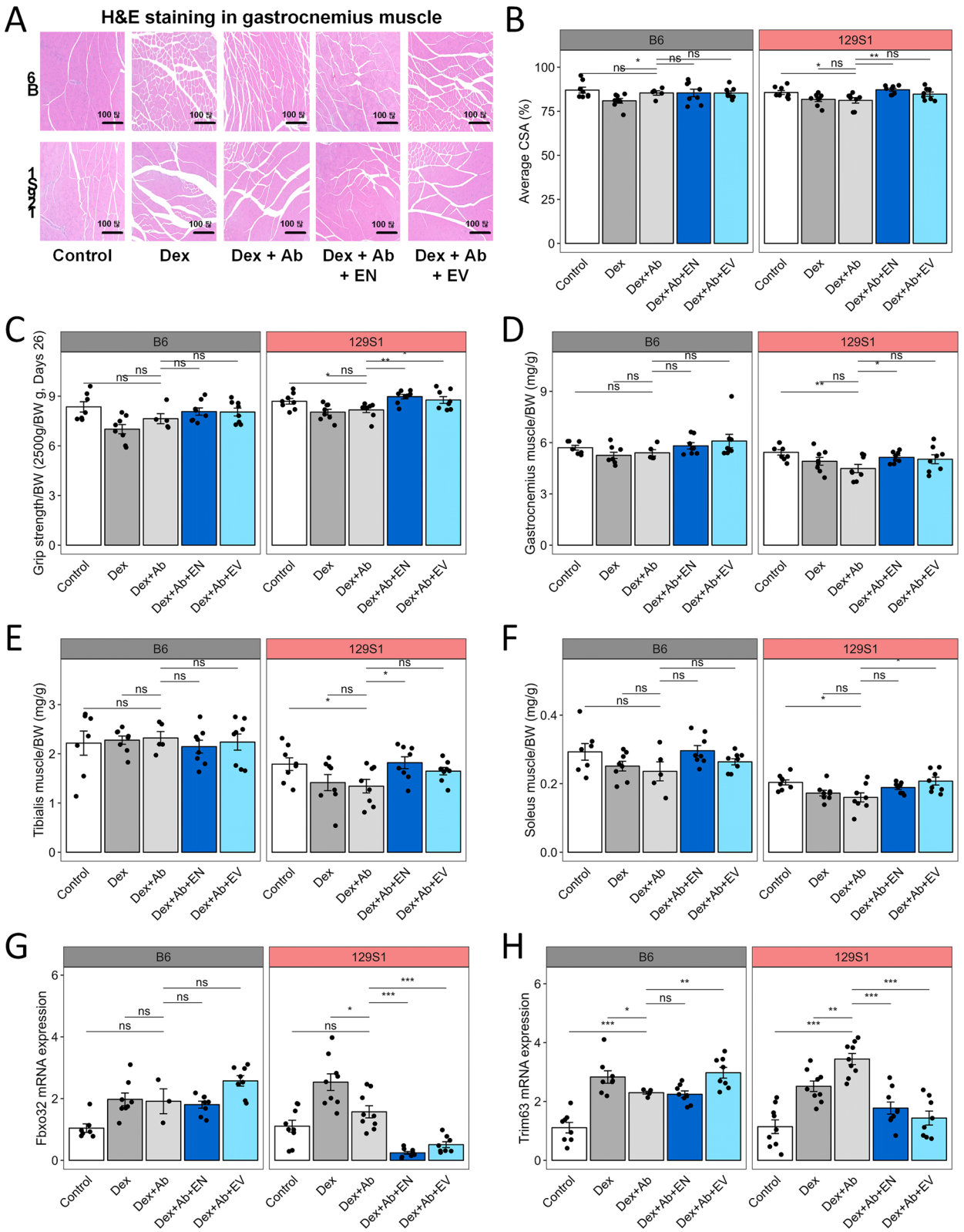

Fig. 4 (See legend on previous page.)

effect of genetic background on the response of these markers to EN and EV administration (Fig. 5G, H). While EV increased the expression of *Alpl* and *Tnfrsf11b* in the 129S1 strain, its effects on these markers were less pronounced in the B6 strain. This further supports the notion that the efficacy of EN and EV in promoting bone health is influenced by the host's genetic background, potentially through their impact on osteoblast differentiation.

EN and EV enhance exercise performance in a strain-specific manner through modulation of mitochondrial biogenesis and gut microbiota

Prior observations indicated strain-specific influences of EN and EV on muscle atrophy and bone health-related traits. We investigated whether their effects on endurance performance and mitochondrial biogenesis in DEX-treated mice are influenced by the host genetic background. In contrast to the limited effects on grip strength and muscle mass in the B6 strain, both EN and EV treatments significantly increased the exercise performance during the treadmill running test in this strain (Fig. 6A). A significant strain effect was observed on the exercise performance (Fig. S6O and P), suggesting a possible genetic influence on endurance capacity. Next, we focused on mitochondrial biogenesis as a potential underlying mechanism for improved exercise performance. EV treatment significantly increased the mRNA expression of *Ppargc1a* (PGC-1α), a key transcriptional co-activator regulating mitochondrial biogenesis, in the tibialis muscle of the B6 strain (Fig. 6B). This upregulation was further reflected in the increased expression of downstream mitochondrial biogenesis markers, including *Tfam*, *Tomm20*, and *Nrf1* (Figs. 6C, S7G, S7H). These findings suggest that EN and EV enhance endurance capacity in B6 mice by promoting mitochondrial biogenesis through PGC-1α signaling.

Building on the observed improvements in exercise performance and mitochondrial biogenesis following EN and EV treatments in the B6 strain, we investigated their effects on the gut microbiome of DEX-treated mice using 16S rRNA gene amplicon sequencing of fecal samples. Given the established link between the gut microbiota and exercise performance in humans and genetically diverse mice [37–39], we hypothesized that EN and EV might exert their effects through gut microbial modulation. Compared with the control group, DEX and antibiotic pretreatment had a minimal impact on the gut microbiota composition in the 129S1 strain (phylum and class levels) (Fig. 6D and E). However, in the B6 strain, DEX and antibiotic pretreatment significantly increased the relative abundance of *Gammaproteobacteria* and decreased that of *Clostridia* compared with the control group. Notably, EN and EV treatments reversed these DEX-induced changes in the B6 strain (Fig. 6E). DEX and antibiotic pretreatment significantly reduced the alpha diversity indices (observed ASVs and Faith's PD) in both strains (Fig. 6F and G). Interestingly, EV treatment significantly increased these alpha diversity indices in the B6 strain but not in the 129S1 strain (Fig. 6F and G). Additionally, EV treatment displayed a distinct beta diversity profile (Bray–Curtis distance, $p = 0.059$) compared to the DEX and antibiotic groups (Fig. 5H), indicating a shift in the overall gut microbial community composition in the B6 strain following EV administration.

We further explored the association between bacterial genera and exercise performance for each strain. Among the 41 genera identified in at least 10% of the samples, EN or EV treatment significantly increased the abundances of *Romboutsia*, *Rikenella*, and *Lachnoclostridium* specifically in the B6 strain, with minimal changes observed in 129S1 strain (Fig. 6I–K). Furthermore, these bacteria exhibited a significant correlation with endurance-related traits only in the B6 strain (Figs. 6L–N and S9). These findings suggest that EN and EV may enhance exercise performance in B6 mice, potentially through promoting the abundance of specific bacterial taxa, such as short-chain fatty acid (SCFA) producers.

Discussion

This study investigated the complex interplay between host genetics, gut microbiota, and the development of osteosarcopenia. Using a six-strain mouse model, we observed significant interactions between host genetics and gut microbiota, influencing disease phenotypes and responsiveness to Rg3, a phytochemical with potential therapeutic effects. Notably, Rg3 treatment modulated the abundance of specific gut microbes, particularly EN and EV, which were selected for further investigation. To evaluate the therapeutic potential of EN and EV, we

(See figure on next page.)

Fig. 5 Effect of EN and EV on bone microarchitecture markers in DEX-treated B6 and 129S1 mice. Microarchitecture was assessed using (**A**) micro-computed tomography in femur, **B** bone mineral density (BMD), **C** bone volume to total volume (BV/TV), **D** serum osteocalcin, **E** trabecular thickness (Tb.Th), **F** trabecular number (Tb.N), **G** and **H** mRNA expression of genes associated with osteoblast differentiation. Data are represented as the mean ± standard error of the mean (SEM). Statistical significance was determined using one-way ANOVA followed by Tukey's post hoc test. Asterisks indicate significance levels: *$p < 0.05$, **$p < 0.01$, ***$p < 0.001$, ns (not significant). C57BL/6 J (B6); 129S1/SvImJ (129S1)

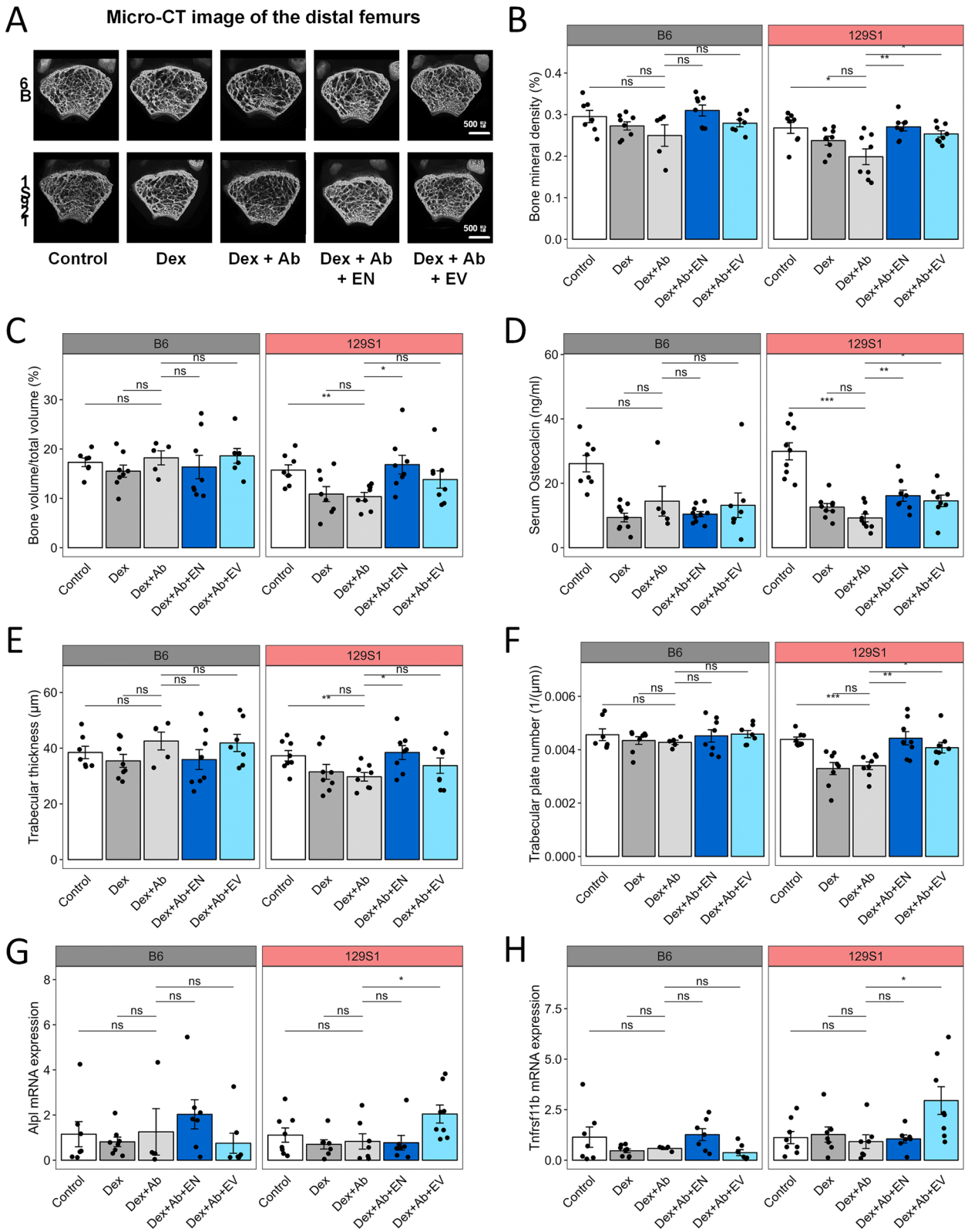

Fig. 5 (See legend on previous page.)

conducted experiments involving oral administration to B6 and 129S1 mouse strains, representing Rg3-responsive and Rg3-unresponsive phenotypes, respectively. These strains were selected due to the observed differences in the effects of Rg3 on their gut microbiota composition. While both strains exhibited muscle atrophy and bone loss following treatment with DEX and antibiotics, oral administration of EN and EV only reversed osteosarcopenic phenotypes in the 129S1 strain. This recovery was evidenced by improvements in grip strength, muscle weight, muscle fiber width, and bone microstructure, suggesting that EN and EV may exert their effects through the modulation of osteoblast differentiation and protein degradation pathways in the 129S1 strain. Interestingly, in the B6 strain, EN and EV modulated mitochondrial biogenesis and microbial diversity but did not significantly improve osteosarcopenic phenotypes. This differential response highlights the complex interplay between host genetics and gut microbiota in determining treatment efficacy.

Consistent with previous reports, 16S rRNA gene amplicon sequencing confirmed substantial variation in the gut microbiota composition at the phylum level across the six CC founder strains [26, 27]. Notably, the abundance of *Verrucomicrobiota* differed significantly, with the wild-derived PWK strain showing the highest abundance and the NOD strain showing the lowest abundance. This observation aligns with our previous findings, in which the PWK strain exhibited superior grip strength, muscle mass, and exercise performance traits among the six strains [25]. In this study, the genus *Akkermansia* was identified as the sole member of the *Verrucomicrobiota* phylum in the mouse strains. Human studies have shown a positive association between *Akkermansia* abundance and bone health, muscle mass, and exercise performance [40, 41]. Additionally, oral administration of *Akkermansia muciniphila* has been shown to alleviate muscle atrophy in mouse models [35, 42]. Overall, these observations suggest that host genetics inherently influence the composition of the resident gut microbiota and that the high abundance of *Akkermansia* in the PWK strain may contribute to its improved osteosarcopenia phenotype.

The present study revealed a significant interaction between Rg3 treatment and host genotype in modulating gut microbiota composition. Notably, Rg3 treatment in the NZO strain, predisposed to obesity, led to a marked reduction in the abundance of *Proteobacteria*, a phylum associated with metabolic disorders and muscle atrophy due to the presence of taxa such as *Escherichia-Shigella* [42, 43]. Conversely, Rg3 treatment increased the abundance of *Verrucomicrobiota* in the PWK strain, likely because of its known ability to promote SCFA-producing bacteria such as *Akkermansia* [44]. These findings highlight the genotype-dependent effects of Rg3 on the gut microbiota composition, which in turn potentially influence its therapeutic efficacy. Beta diversity analysis corroborated these findings, demonstrating a distinct microbial community composition across strains following Rg3 treatment. These observations align with our previous data on the impact of Rg3 treatment on genetic diversity in osteosarcopenia [25] and underscore the intricate interplay between host genetics and treatment outcomes, reinforcing the importance of pharmacogenomics in developing personalized therapeutic strategies [45].

16S rRNA gene amplicon sequencing revealed significant alterations in the gut microbiota composition and diversity within the CC founder strains after Rg3 treatment, with these changes correlating with the osteosarcopenic phenotype. Emerging evidence suggests that alterations in the gut microbiota composition are associated with various disease states [25, 46–48]. Our findings contribute to this growing body of knowledge by shedding light on the intricate interplay between the gut microbiota composition and the modulation of muscle and bone phenotypes in osteosarcopenia. Among the identified microbial modulations, *Akkermansia*, a bacterial genus with documented therapeutic effects on obesity, osteoporosis, and muscle atrophy [35, 31, 49], exhibited a strong positive correlation with Rg3 treatment and improved osteosarcopenic markers in this study. Conversely, the abundance of *Acetatifactor*, a bacterium associated with diabetes, obesity, and inflammatory bowel disease [50–54], was negatively correlated with Rg3 treatment. *Acetatifactor* produces lithocholic

(See figure on next page.)

Fig. 6 Effect of EN and EV on endurance-related markers and gut microbial diversity in DEX-treated mice. **A** Distance to exhaustion, **B**, **C** mRNA expression of (**B**) *Ppargc1a*, and (**C**) *Tfam*. **D**, **E** Relative abundance of bacterial taxa at the (**D**) phylum and (**E**) class levels is displayed in stack bar plot. **F**–**H** Alpha and beta diversity metrics are presented. **F** Observed generate amplicon sequence variants (ASVs), **G** Faith's PD, and (**H**) PCoA plot depicting beta diversity (Bray–Curtis) are shown. **I**–**K** Abundance of specific bacterial genera is presented for (**I**) *Romboutsia*, **J** *Rikenella*, and (**K**) *Lachnoclostridium*. **L**–**N** Spearman correlation coefficients between the abundance of each bacteria genus and time to exhaustion are presented. Data are represented as the mean ± standard error of the mean (SEM). Statistical significance was determined by one-way ANOVA followed by Tukey's post hoc test. Asterisks indicate significance levels: *$p < 0.05$, **$p < 0.01$, ***$p < 0.001$, ns (not significant). C57BL/6 J (B6); 129S1/SvImJ (129S1)

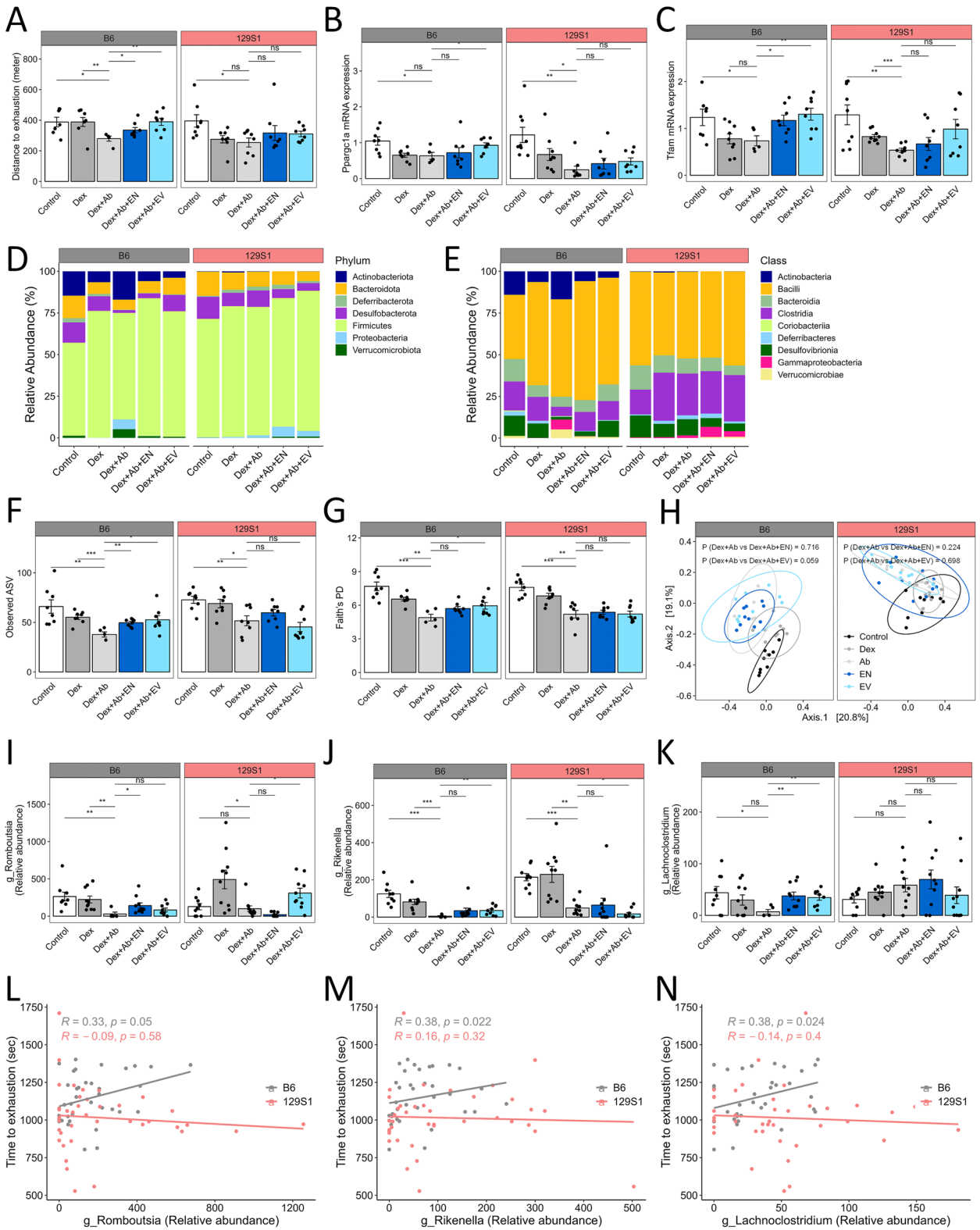

Fig. 6 (See legend on previous page.)

acid, a secondary bile acid that has been implicated in various metabolic and inflammatory disorders [55, 56]. The observed decrease in *Acetatifactor* abundance following Rg3 administration suggests a potential suppressive effect on the production of deleterious bile acids, which could contribute to the observed improvements in osteosarcopenia. However, further investigation is needed to confirm this hypothesis and elucidate the specific mechanisms involved. Our differential abundance analysis using ANCOM identified EN and EV as the bacterial genera consistently modulated by Rg3 treatment across all CC founder strains, independent of the host genotype. Rg3 administration increased the abundance of EN and EV in the fecal and cecal samples, with strain-specific variations. We observed significant positive correlations between EN abundance in fecal samples and grip strength, whereas EV abundance in cecal samples was correlated with grip strength. In addition, the therapeutic potential of EN and EV was shown through the alteration of gene expression and muscle function in B6 and 129S1 mouse strains with DEX- and antibiotic-induced osteosarcopenia. Oral administration of EN and EV modulated the expression of genes associated with protein degradation, myoblast differentiation, and osteoblast differentiation in both strains. These changes subsequently led to the improvement of osteosarcopenic outcomes including muscle mass, grip strength, and bone density. *Eubacterium* is a beneficial bacterial genus known to produce butyrate, an SCFA that contributes to energy metabolism and immune function [57]. Previous studies have reported the enrichment of *Eubacterium* in individuals with regular exercise habits. Conversely, its abundance is diminished in elderly individuals with physical frailty and sarcopenia [58–61]. Furthermore, *Eubacterium* supplementation improves muscle mass, myofiber area, and exercise performance in animal models of muscle atrophy [62, 63]. Interestingly, the abundance of *Eubacterium* has also been linked to both obesity and diabetes, potentially through the activation of PGC-1α signaling [64]. Within the *Eubacterium* genus, EV has been specifically associated with muscle health. Depletion of EV has been observed in patients with muscle atrophy, whereas higher EV abundance has been correlated with greater muscle mass and improved patient survival rates [65–67]. Our findings demonstrated a positive correlation among EN and EV abundance, Rg3 treatment, and the subsequent suppression of osteosarcopenic traits. The results suggest that the suppressive effects of Rg3 on osteosarcopenia may be mediated, at least in part, by the modulation of the gut microbiota, with EN and EV playing key roles.

However, these changes by EN and EV were more pronounced in the 129S1 strain, which also exhibited significant improvements in grip strength, muscle weight, muscle fiber width, and bone microstructure. Interestingly, while the B6 strain showed greater improvement in exercise capacity following EN and EV treatment, this did not correlate with significant improvements in other osteosarcopenic phenotypes. This discrepancy between gene expression changes and phenotypic outcomes, particularly in the B6 strain, highlights the complex interplay between host genetics, gut microbiota, and therapeutic responses. Recent studies have demonstrated that host genetic background can significantly influence the composition and function of the gut microbiota, leading to variations in drug metabolism, nutrient absorption, and immune response [68–71]. For instance, B6 and 129S1 strains exhibit differences in their susceptibility to various diseases and their responses to therapeutic interventions due to variations in their genetic makeup [72–74]. These genetic differences may influence their response to EN and EV, contributing to the observed strain-specific effects. It suggests that while EN and EV may influence certain pathways, their ability to fully reverse osteosarcopenia may be limited by factors specific to the host's genetic background. This underscores the need for further investigation into the mechanisms underlying these strain-specific responses, including a deeper exploration of the pathways involved and the potential influence of other factors, such as host immune response or microbiome composition.

Further analysis revealed that the observed improvement in exercise capacity in the B6 strain may be linked to the modulation of mitochondrial biogenesis. Oral administration of both EN and EV significantly increased PGC-1α mRNA expression, leading to enhanced mitochondrial development [75]. This effect was most pronounced in the B6 strain, mirroring the observed recovery of exercise capacity and gut microbial diversity without the improvement of muscle-related phenotypes. PGC-1α plays a critical role in various metabolic processes, including mitochondrial biogenesis and oxidative metabolism in skeletal muscle [76], contributing to improved mobility and potentially offering a preventive effect against sarcopenia [77, 78]. While the precise relationship between PGC-1α and gut microbiota remains unclear, our findings demonstrate a clear association. Decreased PGC-1α expression has been observed in the intestinal epithelium of patients with inflammatory bowel disease exhibiting gut microbiota abnormalities [79]. Similarly, germ-free and fecal microbiota transplant piglets exhibited downregulated PGC-1α expression in their muscles compared with normal piglets [80]. This suggests that alterations in gut microbiota composition can influence PGC-1α expression and mitochondrial function in various tissues, including skeletal muscle. Furthermore, antibiotic treatment has been shown to decrease exercise

capacity in both humans and DO mice [81]. In this study, antibiotic-induced dysbiosis specifically reduced exercise capacity and PGC-1α expression in the B6 strain. Conversely, EN and EV treatment restored intestinal microbiota in the B6 strain, leading to increased exercise capacity and PGC-1α expression. This suggests that EN and EV may promote mitochondrial biogenesis and enhance exercise capacity, at least in part, by modulating the gut microbiota and restoring microbial diversity. However, further research is needed to elucidate the precise mechanisms underlying these interactions and determine whether similar effects are observed in other genetic backgrounds. Our investigation demonstrates that oral administration of EN and EV alleviates artificially induced osteosarcopenic phenotypes, potentially through upregulation of PGC-1α expression and mitochondrial biogenesis, a mechanism consistent with findings from previous research [82]. However, this effect was primarily observed in the B6 strain, while the 129S1 strain exhibited improvements in muscle and bone health through the modulation of protein degradation and osteoblast differentiation. This further highlights the strain-specific nature of the therapeutic responses to EN and EV.

Our investigation revealed intriguing strain-dependent responses to EN and EV administration in B6 and 129S1 mice, highlighting the complex interplay between host genetics, gut microbiota, and therapeutic responses in osteosarcopenia. While these bacterial strains improved osteosarcopenia-related traits in 129S1 mice, they primarily impacted exercise performance and gut microbiota composition in B6 mice, potentially through the modulation of mitochondrial biogenesis and microbial diversity. This differential response underscores the need for personalized treatment strategies and further research to elucidate the underlying mechanisms. Future studies should investigate the ADME profiles of EN and EV metabolites, examine genetic polymorphisms in relevant pathways, and employ deep metagenomic analysis to better understand the strain-specific effects [83]. Additionally, investigating the host immune response to EN and EV administration in both strains could reveal differences in immune signaling pathways or inflammatory responses that may contribute to the observed strain-specific effects. While this study provides valuable insights, it is important to acknowledge the limitations, such as the use of 16S rRNA sequencing and a mouse model. Future studies should focus on validating these findings in human clinical trials and exploring the specific mechanisms by which EN and EV exert their effects in different genetic backgrounds, including their interactions with host cells and other microbial communities. Overall, this study contributes to our understanding of the complex interplay between host genetics, gut microbiota, and therapeutic responses in osteosarcopenia, paving the way for the development of personalized treatment strategies that consider individual variability in both genetic makeup and gut microbial composition.

Acknowledgements
Not applicable.

Authors' contributions
Concept and design: Choong-Gu Lee, GyHye Yoo, Myungsuk Kim; Supervision: Kwang-Hyun Cha, Young Tae Park, GyHye Yoo, Myungsuk Kim; Resource and material: Soyeon Hong, Bao Ngoc Nguyen, Huitae Min; Data collection and processing: Soyeon Hong, Bao Ngoc Nguyen, Huitae Min, Hye-Young Youn; Analysis/interpretation: Soyeon Hong, Bao Ngoc Nguyen, Myungsuk Kim; Literature search: Soyeon Hong, Bao Ngoc Nguyen, Hye-Young Youn, Myungsuk Kim; Writing: Soyeon Hong, Bao Ngoc Nguyen, Myungsuk Kim. All the authors discussed the results and reviewed the manuscript.

Funding
This research was supported by the Korea Institute of Science and Technology intramural research grants, and a National Research Foundation of Korea (NRF) grant funded by the Korean government (No. NRF-2022R1A6A3A01085975).

Data availability
All sequencing files have been deposited in the NCBI short-read sequence archive (https://www.ncbi.nlm.nih.gov/sra) under BioProject number PRJNA1100731.

Declarations

Ethics approval and consent to participate
All animal experiments were approved by the International Animal Care and Use Committee of the Korea Institute of Science and Technology (Approval no.: KIST-2021–091002; Date of approval: December 30, 2021).

Consent for publication
Not applicable.

Competing interests
The authors declare no competing interests.

Author details
[1]Smart Farm Research Center, Korea Institute of Science and Technology (KIST), Gangneung Institute of Natural Products, Gangneung, Gangwon-Do 25451, Republic of Korea. [2]College of Dentistry, Gangneung Wonju National University, Gangneung, Gangwon-Do, Republic of Korea. [3]Center for Natural Product Efficacy Optimization, Korea Institute of Science and Technology (KIST), Gangneung Institute of Natural Products, 679 Saimdang-Ro, Gangneung, Gangwon-Do 210-340, Republic of Korea. [4]Center for Natural Product Systems Biology, Korea Institute of Science and Technology (KIST) Gangneung Institute, Gangneung 25451, Republic of Korea. [5]Department of Natural Product Applied Science, University of Science and Technology (UST), Daejeon 34113, Republic of Korea. [6]Department of Convergence Medicine, Wonju College of Medicine, Yonsei University, Wonju, Gangwon-Do, Republic of Korea.

Received: 23 May 2024 Accepted: 8 November 2024
Published online: 02 December 2024

References

1. Teng Z, Zhu Y, Teng Y, Long Q, Hao Q, Yu X, et al. The analysis of osteosarcopenia as a risk factor for fractures, mortality, and falls. Osteoporos Int. 2021;32:2173–83. https://doi.org/10.1007/s00198-021-05963-x.
2. Kirk B, Zanker J, Duque G. Osteosarcopenia: epidemiology, diagnosis, and treatment-facts and numbers. J Cachexia Sarcopenia Muscle. 2020;11:609–18. https://doi.org/10.1002/jcsm.12567.

3. Skrzypczak D, Ratajczak AE, Szymczak-Tomczak A, Dobrowolska A, Eder P, Krela-Kaźmierczak I. A vicious cycle of osteosarcopeniain inflammatory bowel diseases-aetiology, clinical implications and therapeutic perspectives. Nutrients. 2021;13. https://doi.org/10.3390/nu13020293.
4. Fagundes Belchior G, Kirk B, da Pereira Silva EA, Duque G. Osteosarcopenia: beyond age-related muscle and bone loss. Eur Geriatr Med. 2020;11:715–24. https://doi.org/10.1007/s41999-020-00355-6.
5. Huang J, Hsu YH, Mo C, Abreu E, Kiel DP, Bonewald LF, et al. METTL21C is a potential pleiotropic gene for osteoporosis and sarcopenia acting through the modulation of the NF-κB signaling pathway. J Bone Miner Res. 2014;29:1531–40. https://doi.org/10.1002/jbmr.2200.
6. Kramer I, Baertschi S, Halleux C, Keller H, Kneissel M. Mef2c deletion in osteocytes results in increased bone mass. J Bone Miner Res. 2012;27:360–73. https://doi.org/10.1002/jbmr.1492.
7. Medina-Gomez C, Kemp JP, Dimou NL, Kreiner E, Chesi A, Zemel BS, et al. Bivariate genome-wide association meta-analysis of pediatric musculoskeletal traits reveals pleiotropic effects at the SREBF1/TOM1L2 locus. Nat Commun. 2017;8:121. https://doi.org/10.1038/s41467-017-00108-3.
8. Papadopoulou SK, Papadimitriou K, Voulgaridou G, Georgaki E, Tsotidou E, Zantidou O et al. Exercise and nutrition impact on osteoporosis and sarcopenia-the incidence of osteosarcopenia: a narrative review. Nutrients. 2021;13. https://doi.org/10.3390/nu13124499.
9. Zhang YW, Song PR, Wang SC, Liu H, Shi ZM, Su JC. Diets intervene osteoporosis via gut-bone axis. Gut Microbes. 2024;16:2295432. https://doi.org/10.1080/19490976.2023.2295432.
10. de Sire A, de Sire R, Curci C, Castiglione F, Wahli W. Role of dietary supplements and probiotics in modulating microbiota and bone health: the gut-bone axis. Cells. 2022;11. https://doi.org/10.3390/cells11040743.
11. Tu Y, Yang R, Xu X, Zhou X. The microbiota-gut-bone axis and bone health. J Leukoc Biol. 2021;110:525–37. https://doi.org/10.1002/JLB.3MR0321-755R.
12. Zhang Y W, Wu Y, Liu X F, Chen X, Su J C. Targeting the gut microbiota-related metabolites for osteoporosis: the inextricable connection of gut-bone axis. Ageing research reviews, 2024;102196. https://doi.org/10.1016/j.arr.2024.102196.
13. Lee K, Kim J, Park SD, Shim JJ, Lee JL. Lactobacillus plantarum HY7715 ameliorates sarcopenia by improving skeletal muscle mass and function in aged Balb/c mice. Int J Mol Sci. 2021;22:10023. https://doi.org/10.3390/ijms221810023.
14. Zhao J, Huang Y, Yu X. A narrative review of gut-muscle axis and sarcopenia: the potential role of gut microbiota. Int J Gen Med. 2021;14:1263–73. https://doi.org/10.2147/IJGM.S301141.
15. Zhang YW, Cao MM, Li YJ, Lu PP, Dai GC, Zhang M. Rui Y F Fecal microbiota transplantation ameliorates bone loss in mice with ovariectomy-induced osteoporosis via modulating gut microbiota and metabolic function. J Orthopaedic Transl. 2022;37:46–60. https://doi.org/10.1016/j.jot.2022.08.003.
16. Lan H, Liu WH, Zheng H, Feng H, Zhao W, Hung WL, Li H. Bifidobacterium lactis BL-99 protects mice with osteoporosis caused by colitis via gut inflammation and gut microbiota regulation. Food Funct. 2022;13:1482–94. https://doi.org/10.1039/d1fo02218k.
17. Fatima M, Brennan-Olsen SL, Duque G. Therapeutic approaches to osteosarcopenia: Insights for the clinician. Ther Adv Musculoskelet Dis. 2019; 11: 1759720X19867009. https://doi.org/10.1177/1759720X19867009.
18. Iglesias-Carres L, Neilson AP. Utilizing preclinical models of genetic diversity to improve translation of phytochemical activities from rodents to humans and inform personalized nutrition. Food Funct. 2021;12:11077–105. https://doi.org/10.1039/d1fo02782d.
19. Svenson KL, Gatti DM, Valdar W, Welsh CE, Cheng R, Chesler EJ, et al. High-resolution genetic mapping using the mouse diversity outbred population. Genetics. 2012;190:437–47. https://doi.org/10.1534/genetics.111.132597.
20. Nagarajan A, Scoggin K, Gupta J, Threadgill DW, Andrews-Polymenis HL. Using the collaborative cross to identify the role of host genetics in defining the murine gut microbiome. Microbiome. 2023;11:149. https://doi.org/10.1186/s40168-023-01552-8.
21. Gelinas R, Chesler EJ, Vasconcelos D, Miller DR, Yuan Y, Wang K, et al. A genetic approach to the prediction of drug side effects: bleomycin induces concordant phenotypes in mice of the collaborative cross. Pharmgenomics Pers Med. 2011;4:35–45. https://doi.org/10.2147/PGPM.S22475.
22. Masson SWC, Madsen S, Cooke KC, Potter M, Vegas AD, Carroll L, et al. Leveraging genetic diversity to identify small molecules that reverse mouse skeletal muscle insulin resistance. eLife. 2023;12. https://doi.org/10.7554/eLife.86961.
23. Mosedale M. Mouse population-based approaches to investigate adverse drug reactions. Drug Metab Dispos. 2018;46:1787–95. https://doi.org/10.1124/dmd.118.082834.
24. Griffin LE, Essenmacher L, Racine KC, Iglesias-Carres L, Tessem JS, Smith SM, et al. Diet-induced obesity in genetically diverse collaborative cross mouse founder strains reveals diverse phenotype response and amelioration by quercetin treatment in 129S1/SvImJ, PWK/EiJ, CAST/PhJ, and WSB/EiJ mice. J Nutr Biochem. 2021;87:108521. https://doi.org/10.1016/j.jnutbio.2020.108521.
25. Nguyen B. N, Hong S, Choi S, Lee CG, Yoo G, Kim M Dexamethasone-induced muscle atrophy and bone loss in six genetically diverse collaborative cross founder strains demonstrates phenotypic variability by Rg3 treatment. J Ginseng Res. 2024;48(3):310–22. https://doi.org/10.1016/j.jgr.2023.12.004.
26. Safari SZ, Bruneau A, Monnoye M, Mariadassou M, Philippe C, Zatloukal K et al. Murine genetic background overcomes gut microbiota changes to explain metabolic response to high-fat diet. Nutrients. 2020;12. https://doi.org/10.3390/nu12020287.
27. Kemis JH, Linke V, Barrett KL, Boehm FJ, Traeger LL, Keller MP, et al. Genetic determinants of gut microbiota composition and bile acid profiles in mice. PLOS Genet. 2019;15:e1008073. https://doi.org/10.1371/journal.pgen.1008073.
28. Shi L, Luo J, Wei X, Xu X, Tu L. The protective role of ginsenoside Rg3 in heart diseases and mental disorders. Front Pharmacol. 2024;15:1327033. https://doi.org/10.3389/fphar.2024.1327033.
29. Wang J, Zeng L, Zhang Y, Qi W, Wang Z, Tian L, et al. Pharmacological properties, molecular mechanisms and therapeutic potential of ginsenoside Rg3 as an antioxidant and anti-inflammatory agent. Front Pharmacol. 2022;13:975784. https://doi.org/10.3389/fphar.2022.975784.
30. Lozupone C, Knight R. UniFrac: a new phylogenetic method for comparing microbial communities. Appl Environ Microbiol. 2005;71:8228–35. https://doi.org/10.1128/AEM.71.12.8228-8235.2005.
31. McMurdie PJ, Holmes S. phyloseq: an R package for reproducible interactive analysis and graphics of microbiome census data. PLoS One. 2013;8:e61217. https://doi.org/10.1371/journal.pone.0061217.
32. Kolde R, Franzosa EA, Rahnavard G, Hall AB, Vlamakis H, Stevens C, et al. Host genetic variation and its microbiome interactions within the human microbiome project. Genome Med. 2018;10:6. https://doi.org/10.1186/s13073-018-0515-8.
33. Kaul A, Mandal S, Davidov O, Peddada SD. Analysis of microbiome data in the presence of excess zeros. Front Microbiol. 2017;8:2114. https://doi.org/10.3389/fmicb.2017.02114.
34. Oksanen J, Blanchet FG, Friendly M, Kindt R, Legendre P, McGlinn D, et al., 2018. vegan: community ecology package. R package version 2.5–2. https://CRAN.R-project.org/package=vegan.
35. Byeon HR, Jang SY, Lee Y, Kim D, Hong MG, Lee D, et al. New strains of Akkermansia muciniphila and Faecalibacterium prausnitzii are effective for improving the muscle strength of mice with immobilization-induced muscular atrophy. J Med Food. 2022;25:565–75. https://doi.org/10.1089/jmf.2021.K.0148.
36. Taylor SA, Green RM. Bile acids, microbiota, and metabolism. Hepatology. 2019;68(4):1229–31. https://doi.org/10.1002/hep.30078.
37. O'Brien MT, O'Sullivan O, Claesson MJ, Cotter PD. The athlete gut microbiome and its relevance to health and performance: a review. Sports Med. 2022;52(Suppl 1):119–28. https://doi.org/10.1007/s40279-022-01785-x.
38. Clauss M, Gérard P, Mosca A, Leclerc M. Interplay between exercise and gut microbiome in the context of human health and performance. Front Nutr. 2021;8:637010. https://doi.org/10.3389/fnut.2021.637010.
39. Dohnalová L, Lundgren P, Carty JRE, Goldstein N, Wenski SL, Nanudorn P, et al. A microbiome-dependent gut-brain pathway regulates motivation for exercise. Nature. 2022;612:739–47. https://doi.org/10.1038/s41586-022-05525-z.
40. Jian H, Liu Y, Wang X, Dong X, Zou X. Akkermansia muciniphila as a next-generation probiotic in modulating human metabolic homeostasis and disease progression: a role mediated by gut-liver-brain axes? Int J Mol Sci. 2023;24. https://doi.org/10.3390/ijms24043900.

41. Okoro PC, Orwoll ES, Huttenhower C, Morgan X, Kuntz TM, McIver LJ, et al. A two-cohort study on the association between the gut microbiota and bone density, microarchitecture, and strength. Front Endocrinol (Lausanne). 2023;14:1237727. https://doi.org/10.3389/fendo.2023.1237727.
42. Grajeda-Iglesias C, Durand S, Daillère R, Iribarren K, Lemaitre F, Derosa L, et al. Oral administration of Akkermansia muciniphila elevates systemic antiaging and anticancer metabolites. Aging (Albany NY). 2021;13:6375–405. https://doi.org/10.18632/aging.202739.
43. Rizzatti G, Lopetuso LR, Gibiino G, Binda C, Gasbarrini A. Proteobacteria: a common factor in human diseases. BioMed Res Int. 2017;2017:9351507. https://doi.org/10.1155/2017/9351507.
44. Wang G, Liu J, Zhang Y, Xie J, Chen S, Shi Y, et al. Ginsenoside Rg3 enriches SCFA-producing commensal bacteria to confer protection against enteric viral infection via the cGAS-STING-type I IFN axis. ISME J. 2023;17:2426–40. https://doi.org/10.1038/s41396-023-01541-7.
45. Schwab M, Schaeffeler E. Pharmacogenomics: a key component of personalized therapy. Genome Med. 2012;4:93. https://doi.org/10.1186/gm394.
46. Durack J, Lynch SV. The gut microbiome: relationships with disease and opportunities for therapy. J Exp Med. 2019;216:20–40. https://doi.org/10.1084/jem.20180448.
47. Chang SC, Lin SF, Chen ST, Chang PY, Yeh YM, Lo FS, et al. Alterations of gut microbiota in patients with Graves' disease. Front Cell Infect Microbiol. 2021;11:663131. https://doi.org/10.3389/fcimb.2021.663131.
48. Genton L, Cani PD, Schrenzel J. Alterations of gut barrier and gut microbiota in food restriction, food deprivation and protein-energy wasting. Clin Nutr. 2015;34:341–9. https://doi.org/10.1016/j.clnu.2014.10.003.
49. Deng L, Ou Z, Huang D, Li C, Lu Z, Liu W, et al. Diverse effects of different Akkermansia muciniphila genotypes on Brown adipose tissue inflammation and whitening in a high-fat-diet murine model. Microb Pathog. 2020;147:104353. https://doi.org/10.1016/j.micpath.2020.104353.
50. Pfeiffer N, Desmarchelier C, Blaut M, Daniel H, Haller D, Clavel T. Acetatifactor muris gen. nov., sp. nov., a novel bacterium isolated from the intestine of an obese mouse. Arch Microbiol. 2012;194:901–7. https://doi.org/10.1007/s00203-012-0822-1.
51. Kim J, Choi JH, Oh T, Ahn B, Unno T. Codium fragile ameliorates high-fat diet-induced metabolism by modulating the gut microbiota in mice. Nutrients. 2020;12. https://doi.org/10.3390/nu12061848.
52. Plovier H, Everard A, Druart C, Depommier C, Van Hul M, Geurts L, et al. A purified membrane protein from Akkermansia muciniphila or the pasteurized bacterium improves metabolism in obese and diabetic mice. Nat Med. 2017;23:107–13. https://doi.org/10.1038/nm.4236.
53. Depommier C, Everard A, Druart C, Plovier H, Van Hul M, Vieira-Silva S, et al. Supplementation with Akkermansia muciniphila in overweight and obese human volunteers: a proof-of-concept exploratory study. Nat Med. 2019;25:1096–103. https://doi.org/10.1038/s41591-019-0495-2.
54. Parada Venegas D, De la Fuente MK, Landskron G, González MJ, Quera R, Dijkstra G, et al. Short chain fatty acids (SCFAs)-mediated gut epithelial and immune regulation and its relevance for inflammatory bowel diseases. Front Immunol. 2019;10:277. https://doi.org/10.3389/fimmu.2019.00277.
55. Taylor SA, Green RM. Bile acids, microbiota, and metabolism. Hepatology. 2018;68:1229–31. https://doi.org/10.1002/hep.30078.
56. Schoeler M, Ellero-Simatos S, Birkner T, Mayneris-Perxachs J, Olsson L, Brolin H, et al. The interplay between dietary fatty acids and gut microbiota influences host metabolism and hepatic steatosis. Nat Commun. 2023;14:5329. https://doi.org/10.1038/s41467-023-41074-3.
57. Mukherjee A, Lordan C, Ross RP, Cotter PD. Gut microbes from the phylogenetically diverse genus Eubacterium and their various contributions to gut health. Gut Microbes. 2020;12:1802866. https://doi.org/10.1080/19490976.2020.1802866.
58. Picca A, Ponziani FR, Calvani R, Marini F, Biancolillo A, Coelho-Junior HJ, et al. Gut microbial, inflammatory and metabolic signatures in older people with physical frailty and sarcopenia: results from the BIOSPHERE study. Nutrients. 2019;12. https://doi.org/10.3390/nu12010065.
59. Kang L, Li P, Wang D, Wang T, Hao D, Qu X. Alterations in intestinal microbiota diversity, composition, and function in patients with sarcopenia. Sci Rep. 2021;11:4628. https://doi.org/10.1038/s41598-021-84031-0.
60. Castellanos N, Diez GG, Antúnez-Almagro C, Bailén M, Bressa C, González Soltero R, et al. A critical mutualism - competition interplay underlies the loss of microbial diversity in sedentary lifestyle. Front Microbiol. 2019;10:3142. https://doi.org/10.3389/fmicb.2019.03142.
61. Palmas V, Pisanu S, Madau V, Casula E, Deledda A, Cusano R, et al. Gut microbiota markers associated with obesity and overweight in Italian adults. Sci Rep. 2021;11:5532. https://doi.org/10.1038/s41598-021-84928-w.
62. Huang WC, Chen YH, Chuang HL, Chiu CC, Huang CC. Investigation of the effects of microbiota on exercise physiological adaption, performance, and energy utilization using a gnotobiotic animal model. Front Microbiol. 2019;10:1906. https://doi.org/10.3389/fmicb.2019.01906.
63. Liu Y, Guo Y, Liu Z, Feng X, Zhou R, He Y, et al. Augmented temperature fluctuation aggravates muscular atrophy through the gut microbiota. Nat Commun. 2023;14:3494. https://doi.org/10.1038/s41467-023-39171-4.
64. Yassour M, Lim MY, Yun HS, Tickle TL, Sung J, Song YM, et al. Sub-clinical detection of gut microbial biomarkers of obesity and type 2 diabetes. Genome Med. 2016;8:17. https://doi.org/10.1186/s13073-016-0271-6.
65. Grahnemo L, Nethander M, Coward E, Gabrielsen ME, Sree S, Billod JM, et al. Identification of three bacterial species associated with increased appendicular lean mass: the HUNT study. Nat Commun. 2023;14:2250. https://doi.org/10.1038/s41467-023-37978-9.
66. Hakozaki T, Nolin-Lapalme A, Kogawa M, Okuma Y, Nakamura S, Moreau-Amaru D, et al. Cancer cachexia among patients with advanced non-small-cell lung cancer on immunotherapy: an observational study with exploratory gut microbiota analysis. Cancers (Basel). 2022; 14. https://doi.org/10.3390/cancers14215405.
67. Mercer NSG. GPs should refuse to provide NHS saftercare for private surgery. BMJ. 2022;379:o2652. https://doi.org/10.1136/bmj.o2652.
68. Goodrich JK, Davenport ER, Beaumont M, Jackson MA, Knight R, Ober C, Ley RE. Genetic determinants of the gut microbiome in UK twins. Cell Host Microbe. 2016;19(5):731–43. https://doi.org/10.1016/j.chom.2016.04.017.
69. Zimmermann M, Zimmermann-Kogadeeva M, Wegmann R, Goodman AL. Mapping human microbiome drug metabolism by gut bacteria and their genes. Nature. 2019;570(7762):462–7. https://doi.org/10.1038/s41586-019-1291-3.
70. Kachuri L, Francis SS, Morrison ML, Wendt GA, Bossé Y, Cavazos TB, Witte JS. The landscape of host genetic factors involved in immune response to common viral infections. Genome Med. 2020;12:1–18. https://doi.org/10.1186/s13073-020-00790-x.
71. Odriozola A, González A, Álvarez-Herms J, Corbi F. Host genetics and nutrition. Adv Genet. 2024;111:199–235. https://doi.org/10.1016/bs.adgen.2024.03.001.
72. Balogh SA, McDowell CS, Stavnezer AJ, Denenberg VH. A behavioral and neuroanatomical assessment of an inbred substrain of 129 mice with behavioral comparisons to C57BL/6J mice. Brain Res. 1999;836(1–2):38–48. https://doi.org/10.1016/s0006-8993(99)01586-3.
73. Beamer WG, Donahue LR, Rosen CJ, Baylink DJ. Genetic variability in adult bone density among inbred strains of mice. Bone. 1996;18(5):397–403. https://doi.org/10.1016/8756-3282(96)00047-6.
74. Kübler M, Götz P, Braumandl A, Beck S, Ishikawa-Ankerhold H, Deindl E. Impact of C57BL/6J and SV-129 mouse strain differences on ischemia-induced postnatal angiogenesis and the associated leukocyte infiltration in a murine hindlimb model of ischemia. Int J Mol Sci. 2021;22(21):11795. https://doi.org/10.3390/ijms222111795.
75. Abu Shelbayeh O, Arroum T, Morris S, Busch KB. PGC-1alpha is a master regulator of mitochondrial lifecycle and ROS stress response. Antioxidants (Basel). 2023;12. https://doi.org/10.3390/antiox12051075.
76. Kang C, Li JL. Role of PGC-1alpha signaling in skeletal muscle health and disease. Ann N Y Acad Sci. 2012;1271:110–7. https://doi.org/10.1111/j.1749-6632.2012.06738.x.
77. Wenz T, Rossi SG, Rotundo RL, Spiegelman BM, Moraes CT. Increased muscle PGC-1alpha expression protects from sarcopenia and metabolic disease during aging. Proc Natl Acad Sci U S A. 2009;106:20405–10. https://doi.org/10.1073/pnas.0911570106.
78. Qian L, Zhu Y, Deng C, Liang Z, Chen J, Chen Y, et al. Peroxisome proliferator-activated receptor gamma coactivator-1 (PGC-1) family in physiological and pathophysiological process and diseases. Signal Transduct Target Ther. 2024;9:50. https://doi.org/10.1038/s41392-024-01756-w.
79. Cunningham KE, Vincent G, Sodhi CP, Novak EA, Ranganathan S, Egan CE, et al. Peroxisome proliferator-activated receptor-gamma coactivator

1-alpha (PGC1alpha) Protects against experimental murine colitis. J Biol Chem. 2016;291:10184–200. https://doi.org/10.1074/jbc.M115.688812.
80. Qi R, Sun J, Qiu X, Zhang Y, Wang J, Wang Q, et al. The intestinal microbiota contributes to the growth and physiological state of muscle tissue in piglets. Sci Rep. 2021;11:11237. https://doi.org/10.1038/s41598-021-90881-5.
81. McNamara MP, Cadney MD, Castro AA, Hillis DA, Kallini KM, Macbeth JC, et al. Oral antibiotics reduce voluntary exercise behavior in athletic mice. Behav Processes. 2022;199:104650. https://doi.org/10.1016/j.beproc.2022.104650.
82. Yu C, Du Y, Peng Z, Ma C, Fang J, Ma L, et al. Research advances in crosstalk between muscle and bone in osteosarcopenia (Review). Exp Ther Med. 2023;25:189. https://doi.org/10.3892/etm.2023.11888.
83. Kreznar JH, Keller MP, Traeger LL, Rabaglia ME, Schueler KL, Stapleton DS, Rey FE. Host genotype and gut microbiome modulate insulin secretion and diet-induced metabolic phenotypes. Cell Rep. 2017;18(7):1739–50. https://doi.org/10.1016/j.celrep.2017.01.062.

Publisher's Note